NUMERICAL SIMULATION OF TURBULENT SEPARATED TRANSONIC FLOWS AROUND THE AXISYMMETRIC BODIES

Kudryashov I.Yu., Lutsky A.E.

The work has been sponsored by the RFBR (Grants 14-08-00624, 15-51-50023).

Outline.

- **Numerical problem formulation.**
- **Flow evolution and features comparison between simulation and experiment.**
- **Separation point position evolution with the growth of Mach number.**
- **Pressure distribution comparison between simulation and experiment.**
- **Preliminary results for three-dimensional unsteady simulation.**
- **Summary.**

Background literature

1. **B.N. Dan'kov et al., "Wave Disturbances in Transonic Separation Flows," Izv. RAN, MZhG, No. 6, 153–165, 2006.**
2. **B.N. Dan'kov et al., "Peculiarities of Transonic Flow behind Stern Angle Edge of Overcalliper Cone-Cylindrical Body," Izv. RAN, MZhG, No. 3, 2007.**
3. **B.N. Dan'kov et al., "The Role of Wave Disturbances in Transonic Separation Flows", TsAGI Science Journal, Vol. XLI №2, pp 19-24, 2010.**
4. **I.Yu. Kudryashov, A.E. Lutsky, "Mathematical simulation of turbulent separated transonic flows around the bodies of revolution", Mathematical Models and Computer Simulations Vol. 3, No 6,pp 690-696, 2011.**
5. **Spalart P.R., Allmaras S.R. A one-equation turbulence model for aerodynamic flows // La Recherche Aerospatiale. 1994; 1: 5-21**
6. **Jean Delery, Jean-Paul Dussauge. Some physical aspects of shock wave/boundary layer interactions // Shock Waves, 2009. Vol. 19. N 6. p. 453-468**

Background.

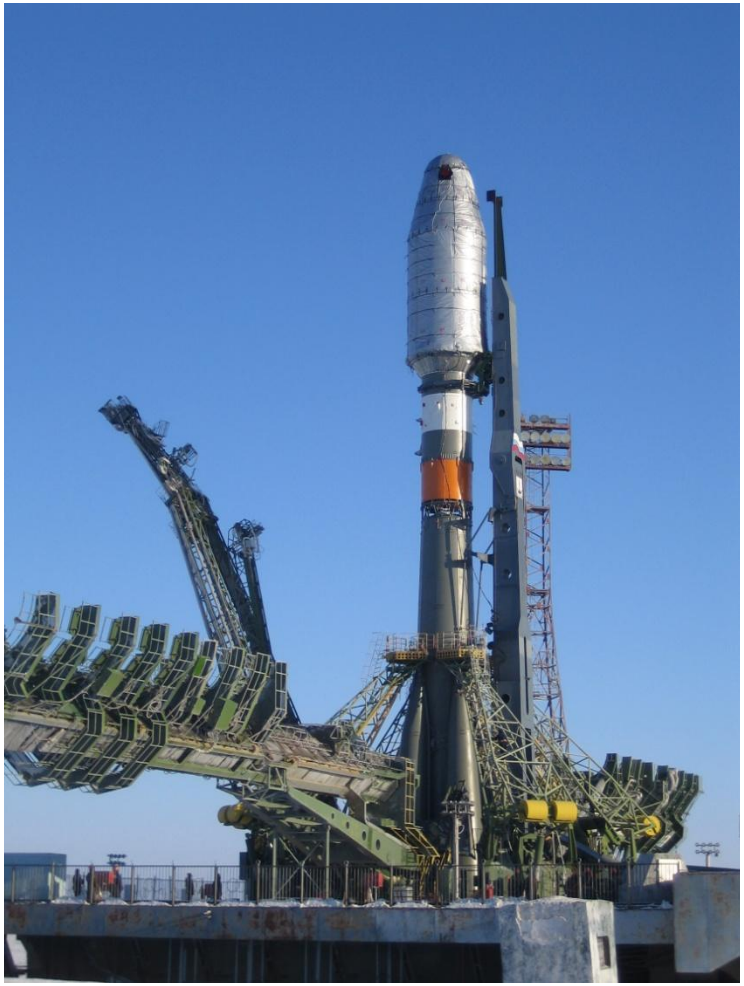

Soyuz-2 booster-vehicle with over-caliber forebody

Numerical problem formulation.

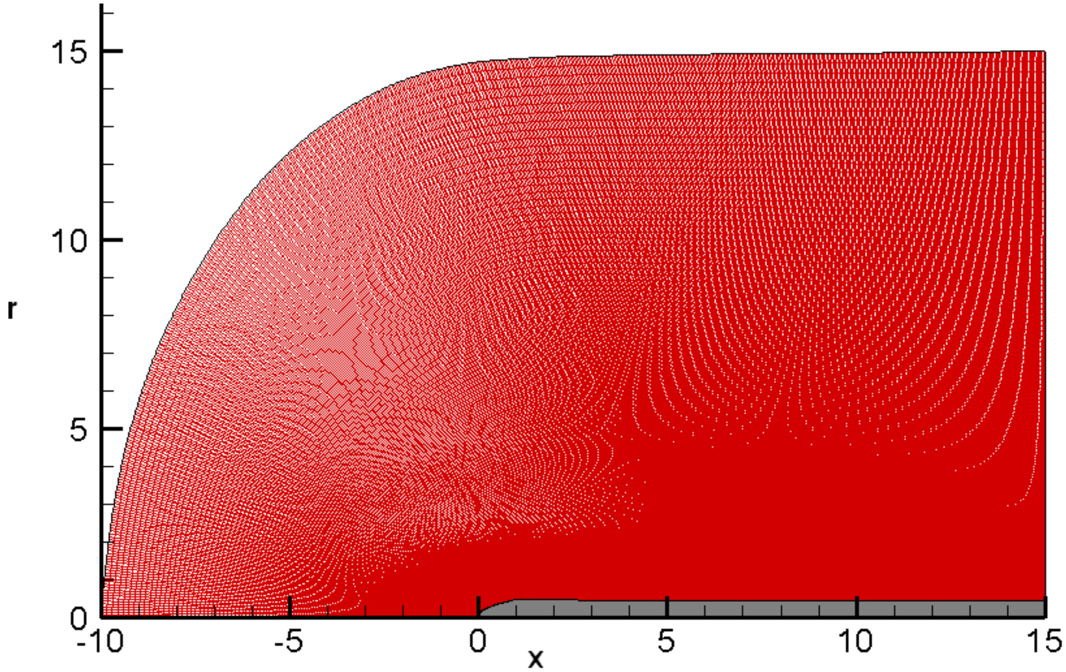

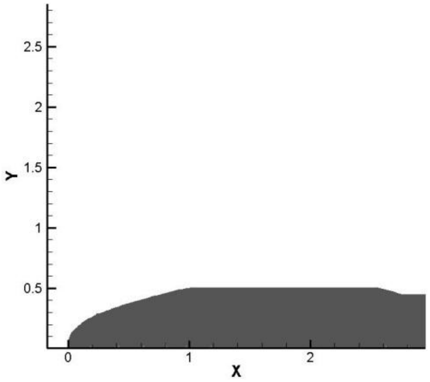

M = 0.82, 0.90, 0.95, 1.1 , $Re=U_\infty D/\nu_\infty$ ~ $3*10^6$ (D – diameter)
Calculations were performed for Euler, Navier–Stokes, and the Reynolds–averaged NS equations coupled with SA and Menter SST turbulence models.

Main flow elements

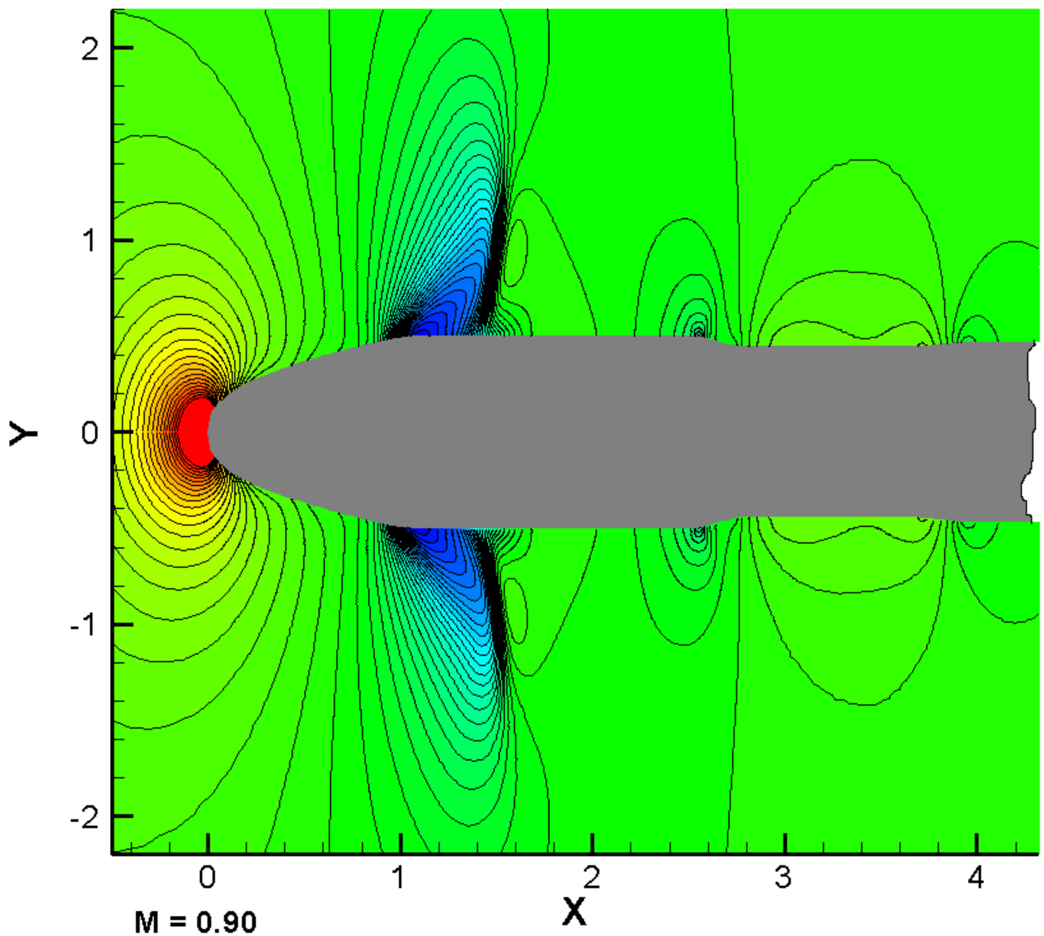

1) Local supersonic domain closed by shock wave
2) shock-wave boundary-layer interaction, and separation on the cylindrical surface
3) Separation bubble on the backward-facing cone

Flow evolution over the cylindrical part

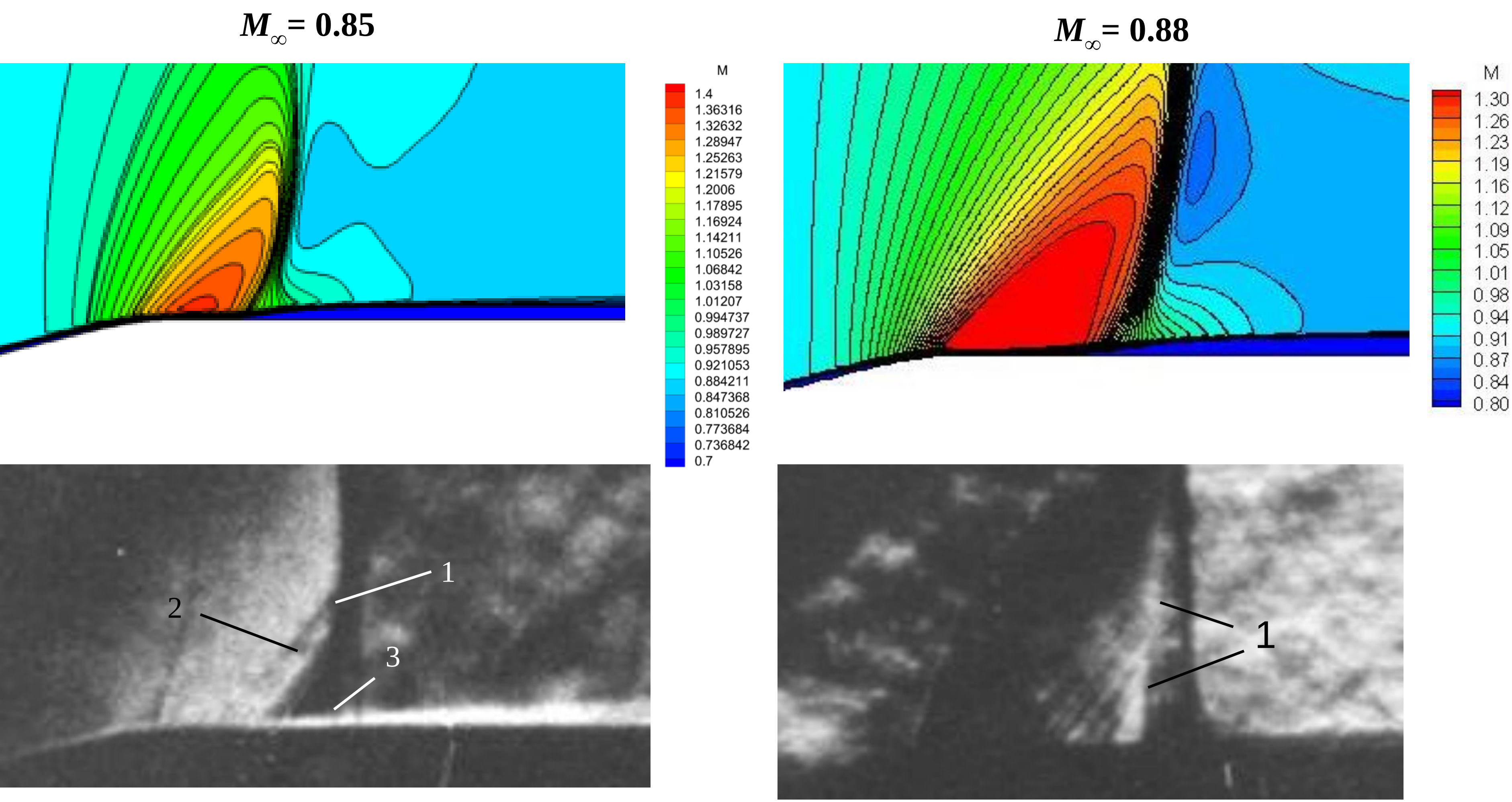

Comparison between numerical fields of local Mach number and experimental Schlieren. 1, 2 – closing and critical shocks; 3, 4 – lateral and aft separation zones; 5 – λ-like shock wave

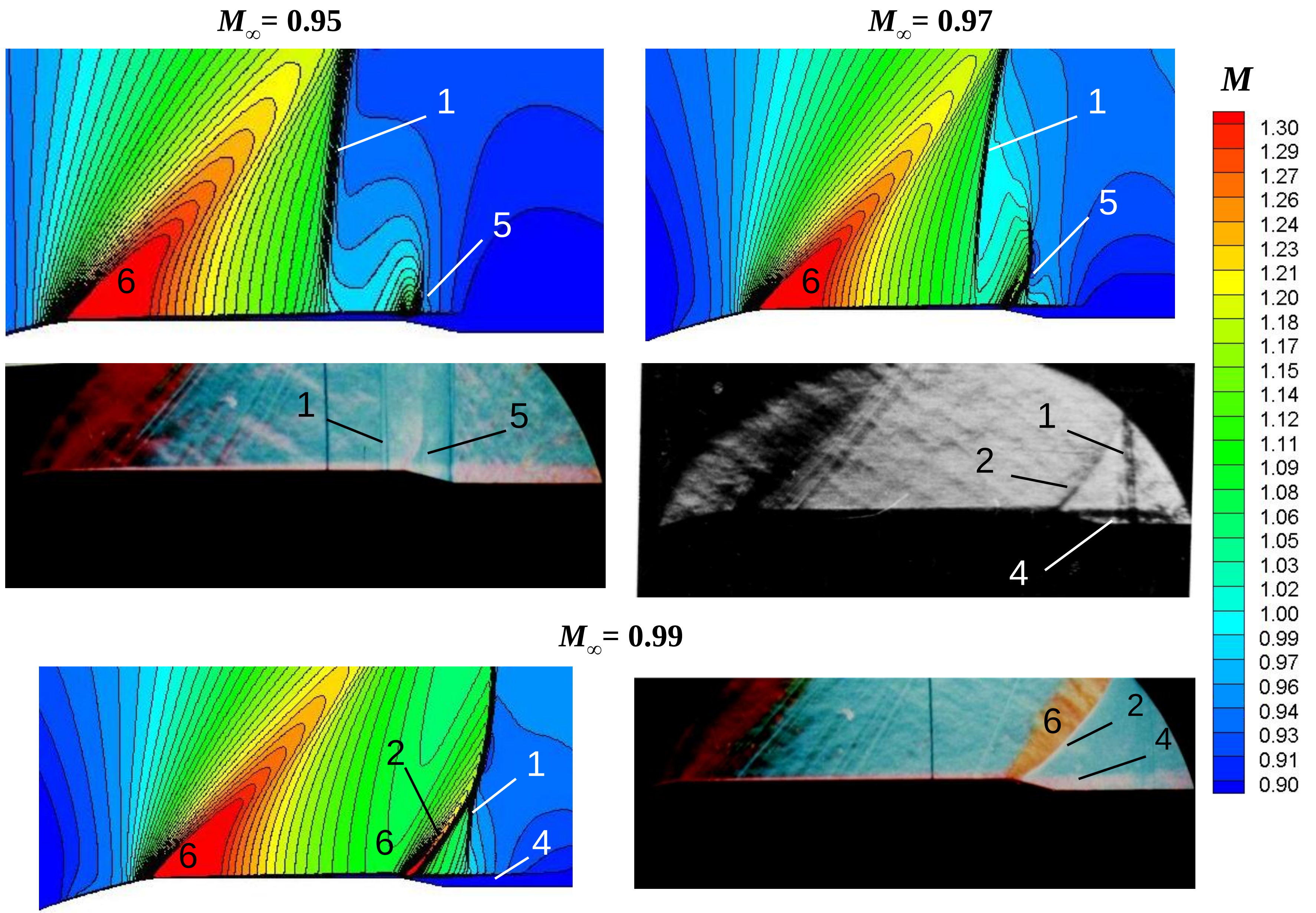

Comparison between numerical fields of local Mach number and experimental Schlieren. 3,4 – lateral and aft separation zones; 5 – λ-like shock wave; 6 – Prandtl–Meyer expansion fan

Evolution of the flow separation over the cylindrical part.

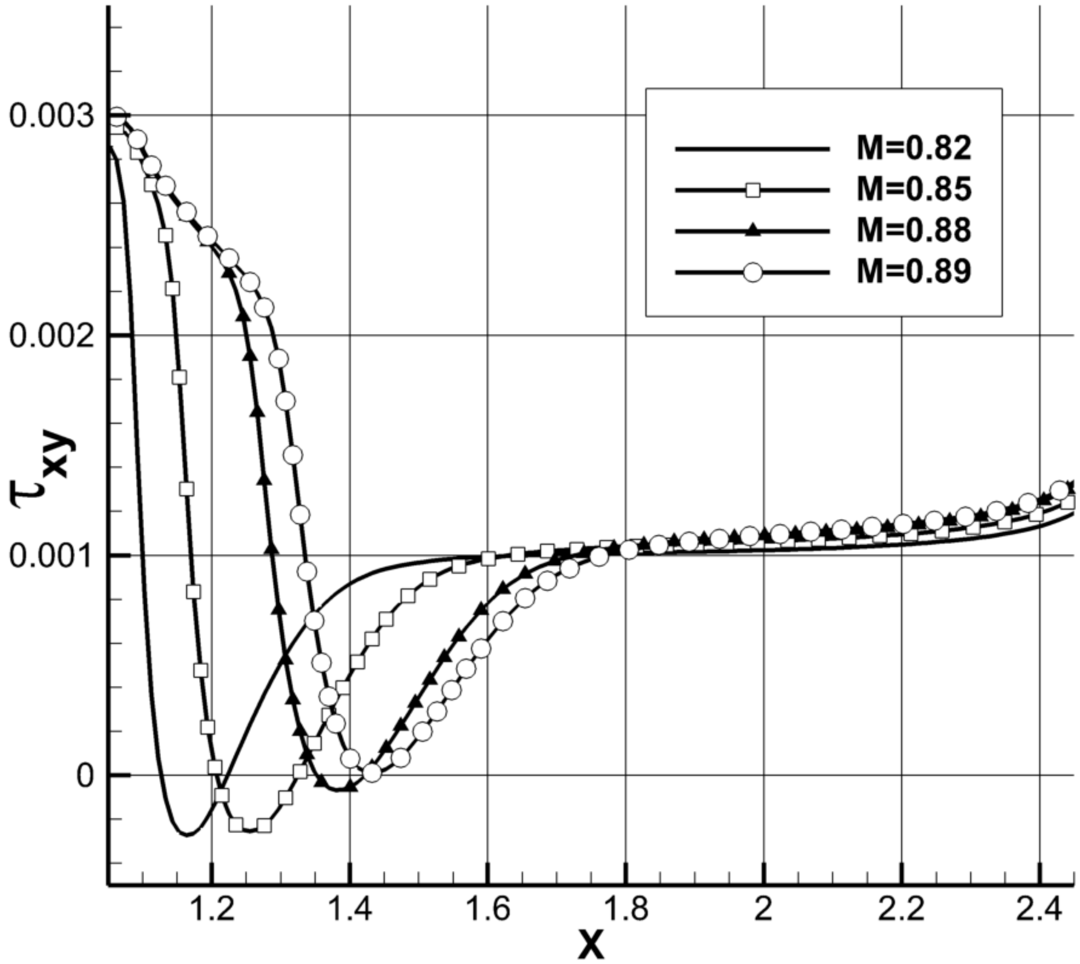

Friction coefficient distribution.

Evolution of the separation point on the backward-facing cone.

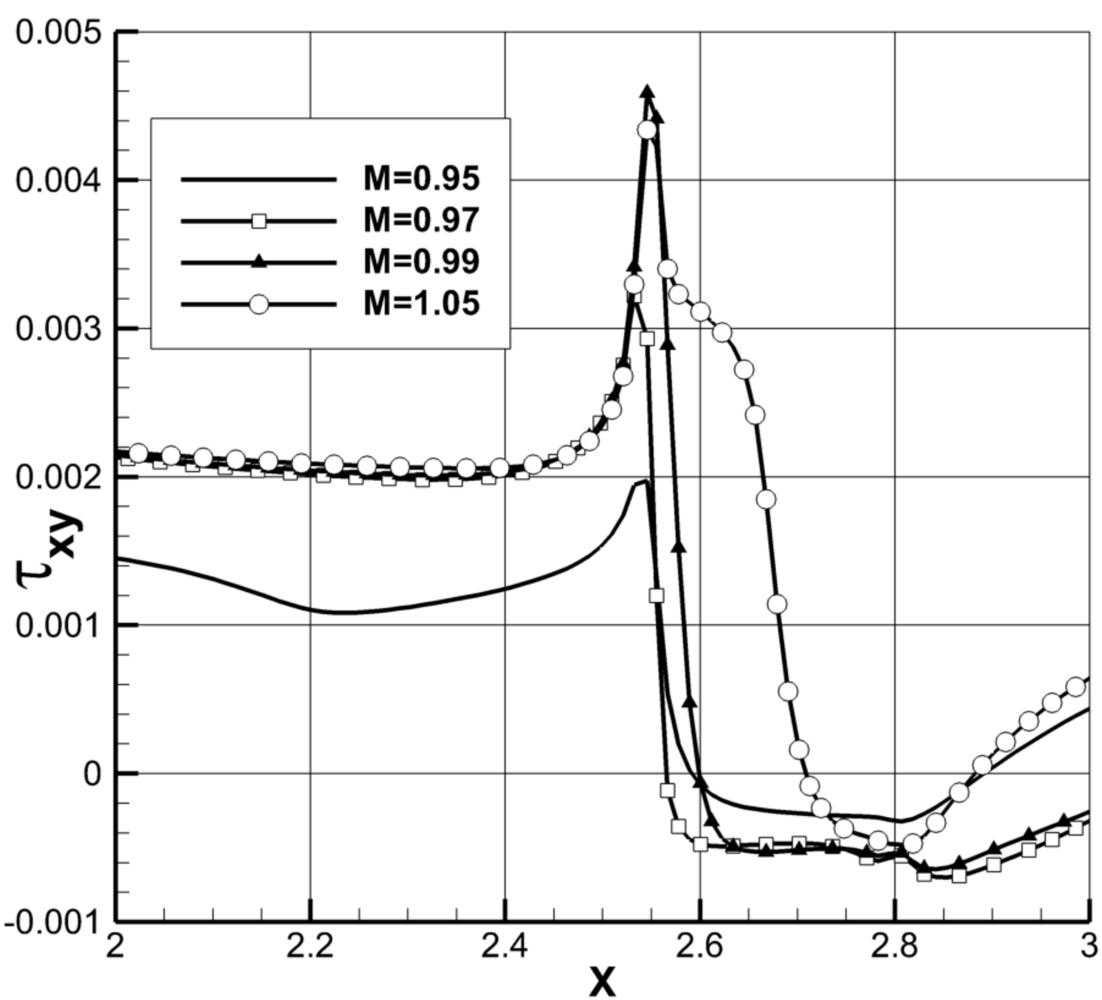

Friction coefficient distribution.

Pressure coefficient distribution.

Experimental data by TsNIIMash [1-4]

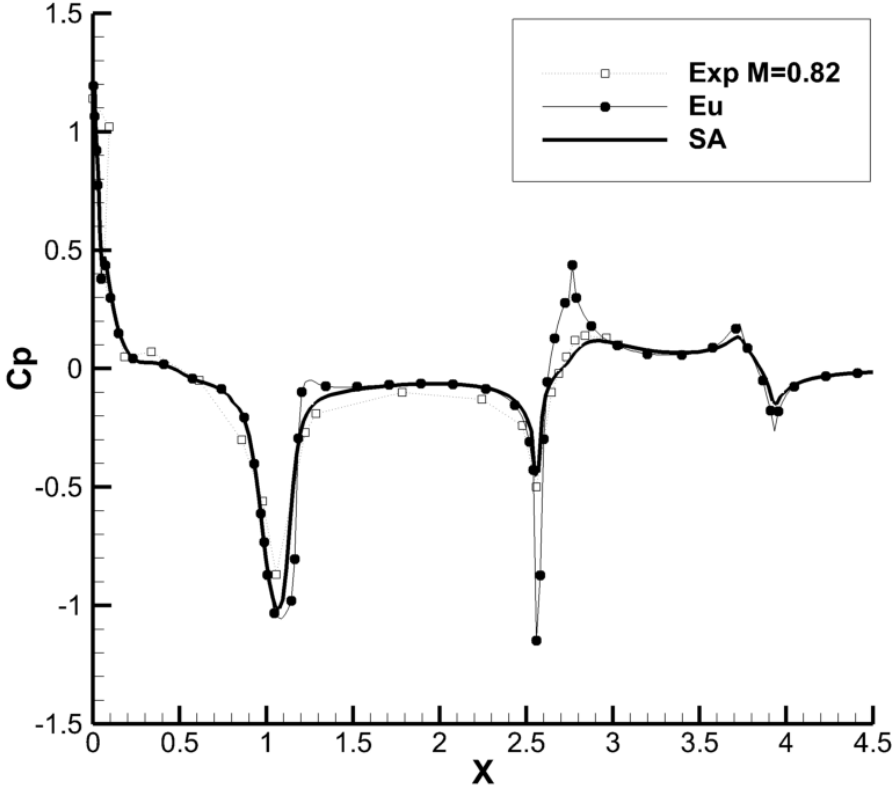

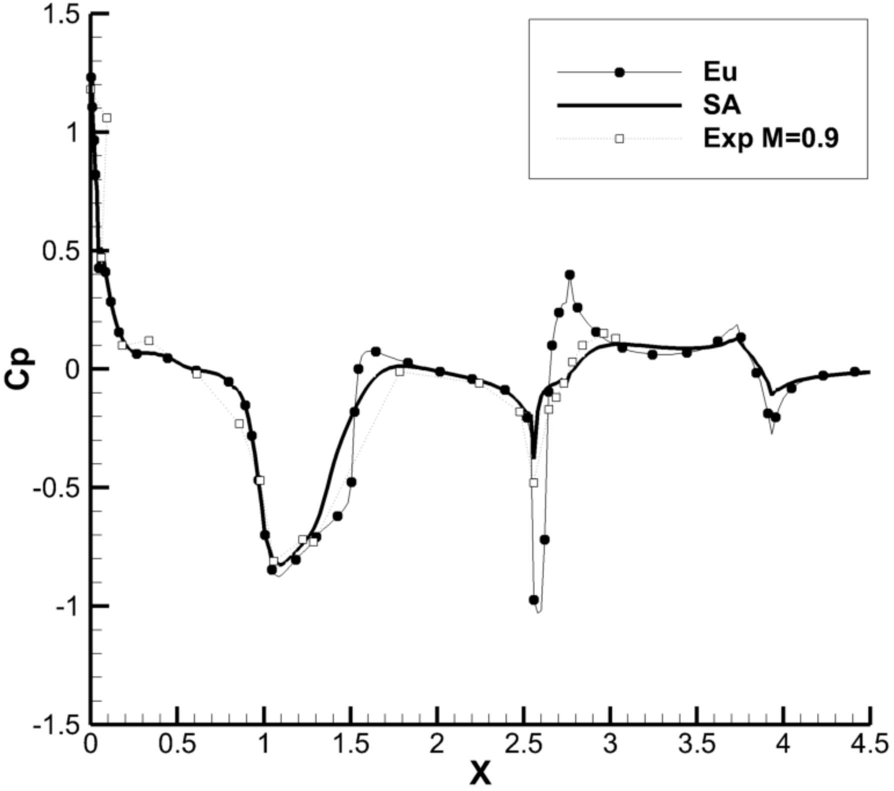

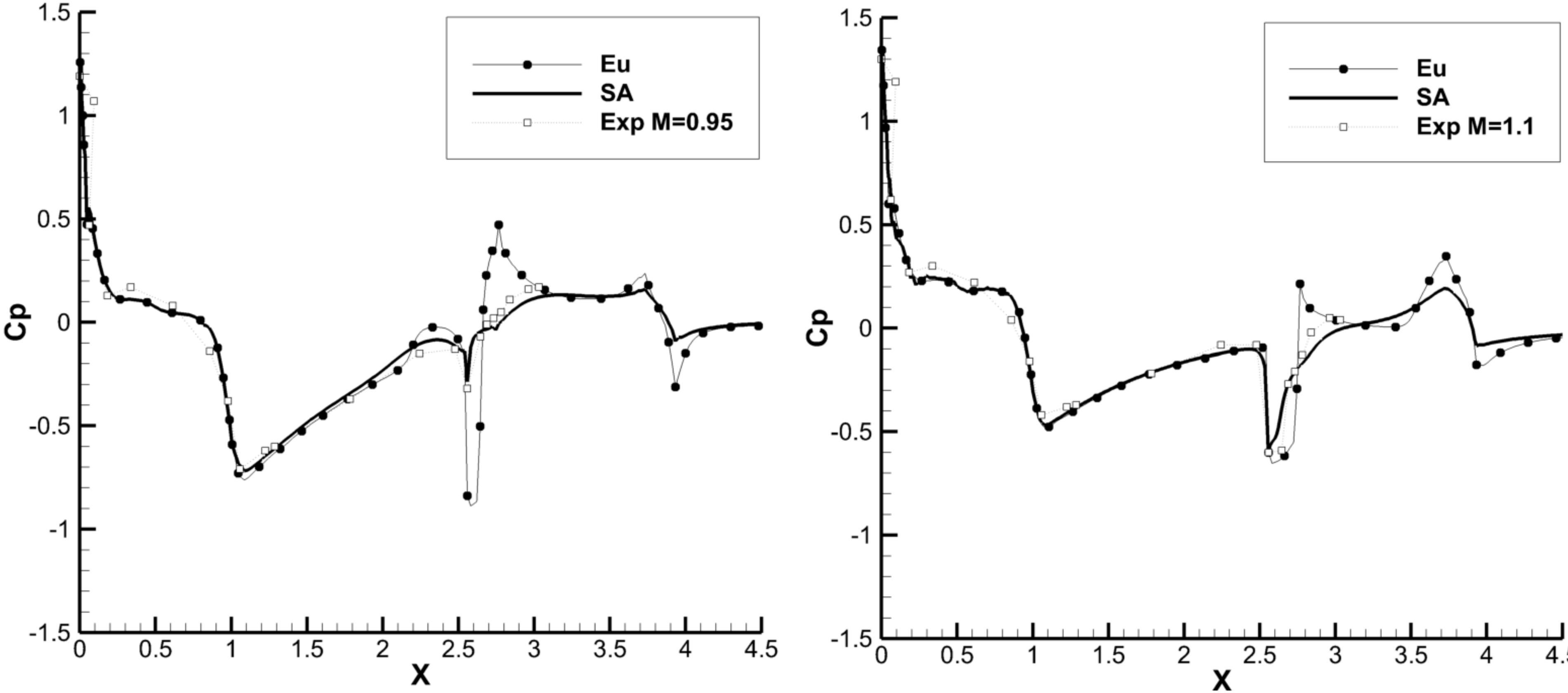

Eu
SA
Exp M=0.95
Cp
X
1.5
1
0.5
0
-0.5
-1
-1.5
0
0.5
1
1.5
2
2.5
3
3.5
4
4.5
Eu
SA
Exp M=1.1
Cp
X

Three-dimensional simulation using MILES method.

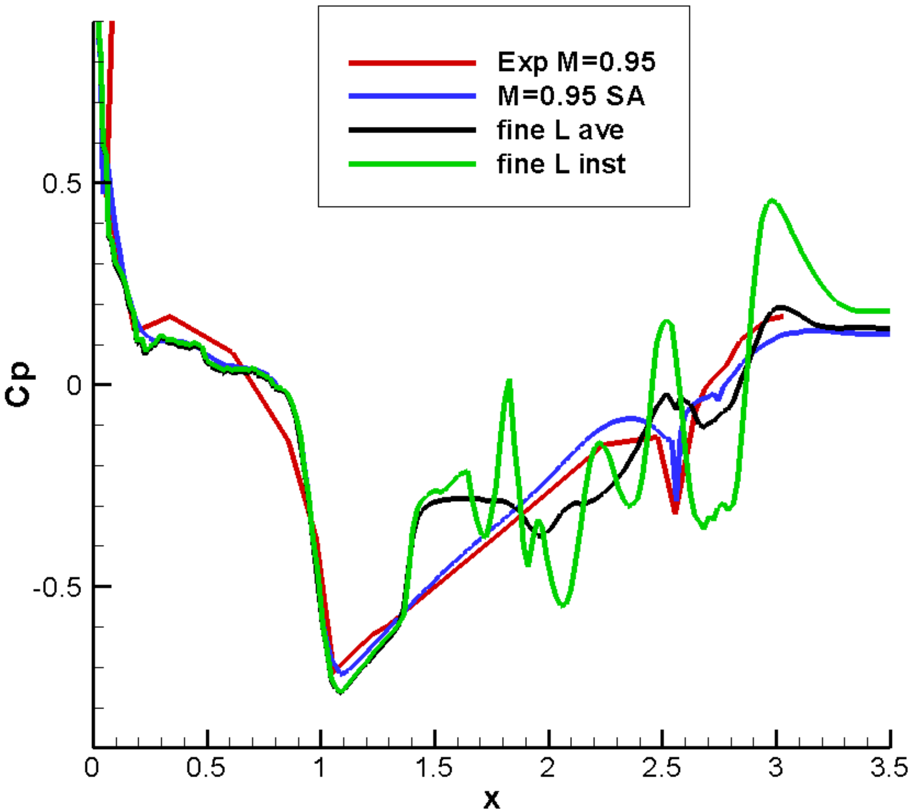

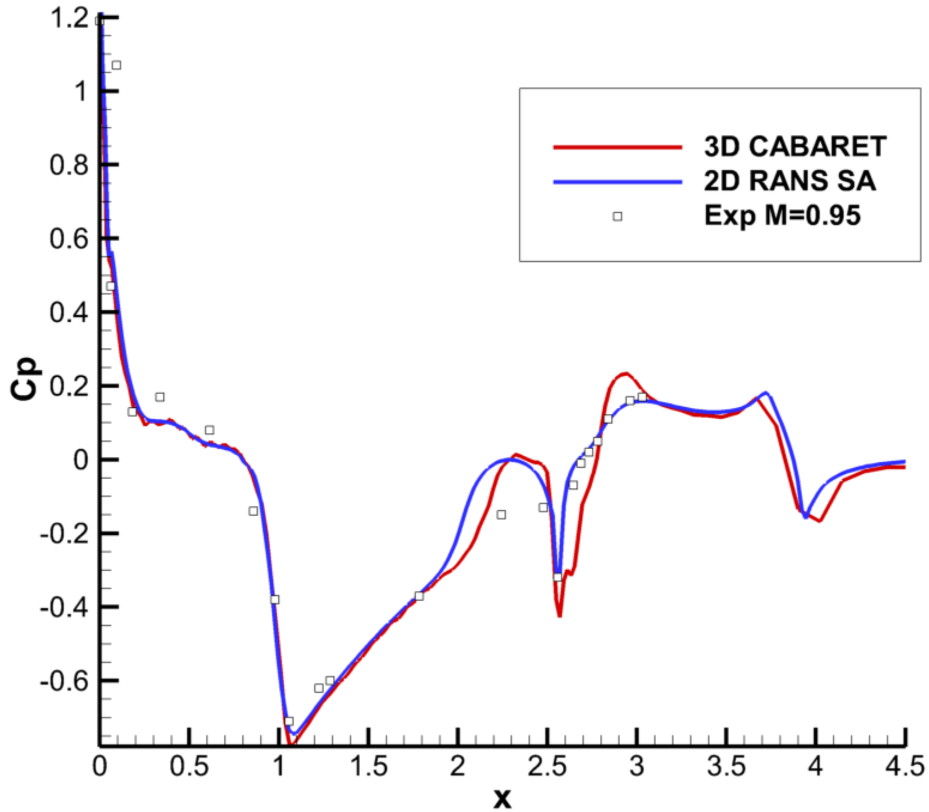

V.A. Semiletov, S.A. Karabasov. **CABARET scheme with conservation-flux asynchronous time-stepping for nonlinear aeroacoustics problems.** J. Comput. Phys., v.253, 2013, pp.157-165.

[Karabasov. Goloviznin, 2009]
[Faranosov et al, 2013]
[Semiletov. Karabasov, 2014]

Unsteady forces

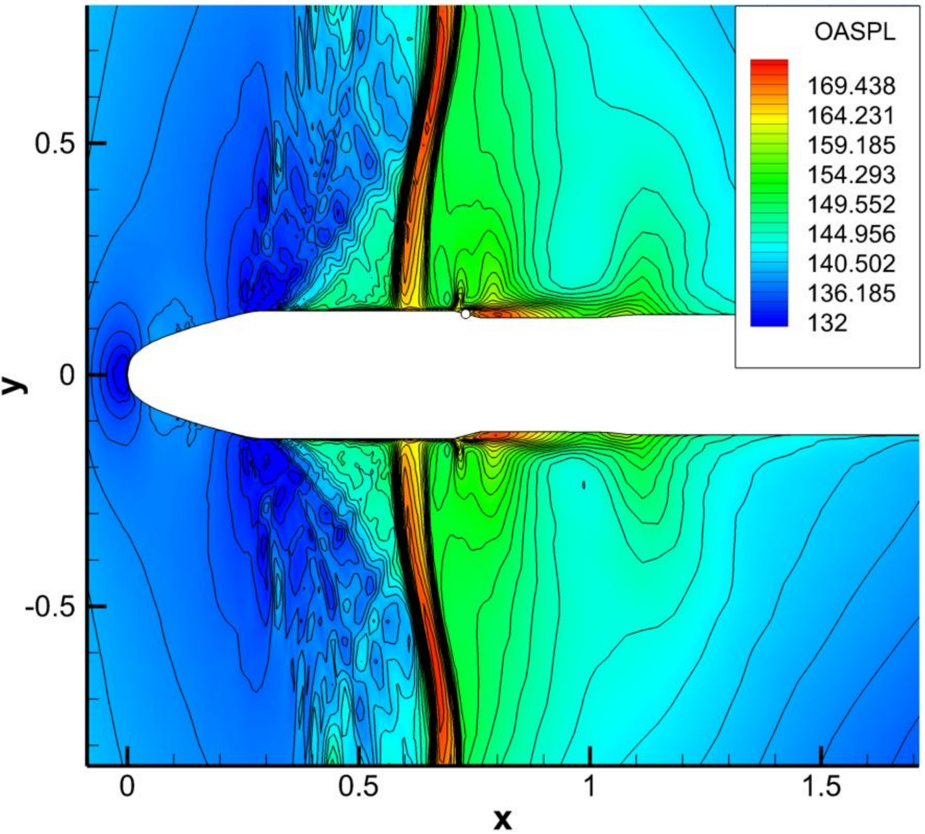

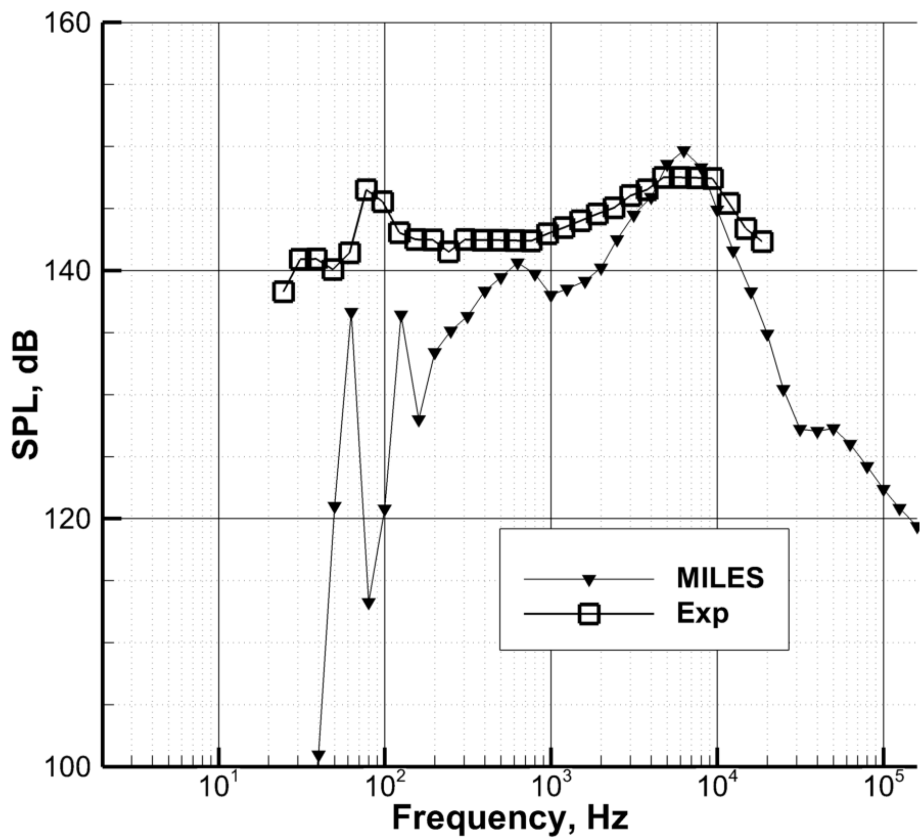

Left: overall sound pressure level distribution;
Right: third octave pressure pulsation spectrum on the backward-facing cone (white circle on the left image). M=0.95

Summary

- Viscosity and turbulence are crucial for accurate numerical modeling of the transonic flow around bodies in question.
- Spalart-Allmaras model deals well with turbulent flow effects in problem under consideration.
- The main features of the transonic flow rearrangement with the growth of Mach number are reproduced in simulation: growth of the local supersonic domain size, transition from the separated to the attached interaction between closing shock and turbulent boundary layer, formation of the separation zone at the backward-facing cone.
- 3D averaged simulation results with MILES are in a good agreement with 2D simulation using RANS. MILES allows one to reveal unsteady nature of the flow and qualitatively reproduce the pressure pulsation spectrum from the experiment.

Thank you for your attention.

Система уравнений

$$\frac{\partial U}{\partial t}+\frac{\partial F}{\partial x}+\frac{\partial G}{\partial y}=H \qquad U=(\rho,\ \rho u,\ \rho v,\ e)^T$$

$$F=F^i+F^v, \qquad G=G^i+G^v, \qquad H=\omega(H^i+H^v)/y$$

$$F^i=\left(\rho u,\rho u^2+p,\rho u\upsilon,(e+p)u\right)^T, \qquad F^v=\left(0,-\tau_{xx},-\tau_{xy},-u\tau_{xx}-\upsilon\tau_{xy}-q_x\right)^T$$

$$G^i=\left(\rho\upsilon,\rho u\upsilon,\rho\upsilon^2+p,(e+p)\upsilon\right)^T, \qquad G^v=\left(0,-\tau_{xy},-\tau_{yy},-u\tau_{xy}-\upsilon\tau_{yy}-q_y\right)^T$$

$$H^i=\left(-\rho\upsilon,-\rho u\upsilon,-\rho\upsilon^2,-(e+p)\upsilon\right)^T, \qquad H^v=\left(0,\tau_{xy},\tau_{yy}-\tau_{\varphi\varphi},u\tau_{xy}+\upsilon\tau_{yy}+q_y\right)^T$$

$\omega=$ (0 – в плоском случае, 1 - в осесимметричном).

$$\tau_{xx}=\frac{2}{3}(\mu+\mu_t)\left(2u_x-v_y-\omega v/y\right) \qquad \tau_{xy}=\tau_{yx}=(\mu+\mu_t)\left(u_y+v_x\right)$$

$$\tau_{yy}=\frac{2}{3}(\mu+\mu_t)\left(2v_y-u_x-\omega v/y\right) \qquad \tau_{\varphi\varphi}=2(\mu+\mu_t)(2v/y-u_x-v_y\})$$

Модель турбулентности

Для определения турбулентной вязкости используется модель Спаларта-Алмараса, добавляющая одно уравнение переноса:

$$\frac{\partial}{\partial t}\left(\rho\tilde{\nu}\right)+\frac{\partial}{\partial x_i}\left(\rho\tilde{\nu}u_i\right)=C_{b1}\rho\tilde{S}\tilde{\nu}+\frac{1}{\sigma_{\tilde{\nu}}}\frac{\partial}{\partial x_j}\left[\left(\mu+\rho\tilde{\nu}\right)\frac{\partial\tilde{\nu}}{\partial x_j}\right]+\frac{C_{b2}\rho}{\sigma_{\tilde{\nu}}}\left(\frac{\partial\tilde{\nu}}{\partial x_j}\right)^2-C_{w1}\rho f_w\frac{\tilde{\nu}^2}{d^2}$$

$$\tilde{S}=S+\frac{\tilde{\nu}}{\kappa^2 d^2}f_{v2} \qquad f_{v1}=\frac{\chi^3}{\chi^3+C_{v1}^3} \qquad f_{v2}=1-\frac{\chi}{1+\chi f_{v1}} \qquad f_w=g\left[\frac{1+C_{w3}^6}{g^6+C_{w3}^6}\right]^{1/6}$$

$$S=\sqrt{2\Omega_{ij}\Omega_{ij}} \qquad \Omega_{ij}=\frac{1}{2}\left(\frac{\partial u_i}{\partial x_j}-\frac{\partial u_j}{\partial x_i}\right)$$

$$g=r+C_{w2}\left(r^6-r\right) \qquad r=\frac{\tilde{\nu}}{\tilde{S}\kappa^2 d^2}$$

C_{v1}=7.1, C_{w2}=0.3, C_{w3}=2., κ=0.41

$$C_{w1}=\frac{C_{b1}}{\kappa^2}+\frac{1+C_{b2}}{\sigma_{\tilde{\nu}}} \qquad \sigma_{\tilde{\nu}}=2/3 \qquad \chi=\frac{\tilde{\nu}}{\nu} \qquad \mu_t=f_{v1}\rho\tilde{\nu}$$

Анализ данных по пульсациям давления

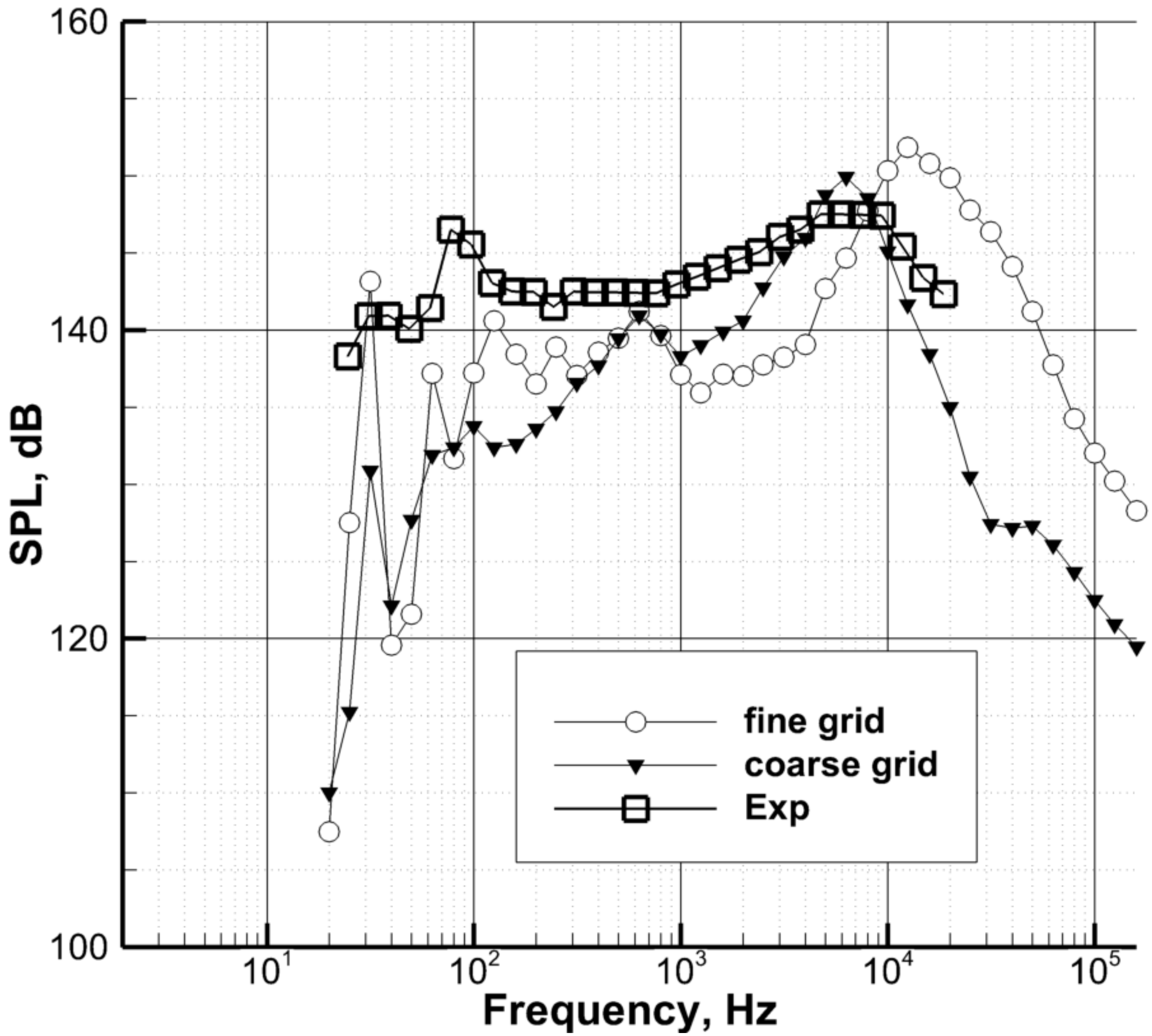

Третьоктавный спектр пульсаций давления; датчик на обратном скате; сравнение с экспериментом для M=0.95.

Алгоритм

$$\Omega\frac{U^{n+1}_{k+1/2,l+1/2}-U^{n}_{k+1/2,l+1/2}}{\Delta t}+\sum_{i=1}^{4}(FN_x+GN_y)_i=\Omega H$$

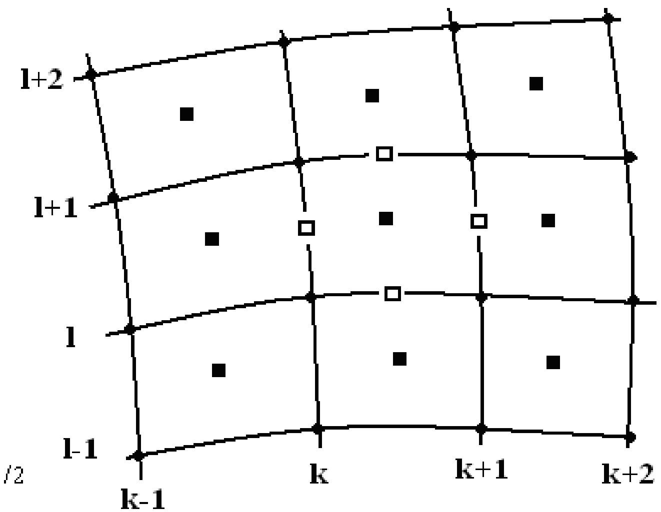

$$U^{+}_{k+1}=U_{k+1/2,l+1/2}+1/2\Delta x U_{x,k+1/2,l+1/2}+1/2\Delta y U_{y,k+1/2,l+1/2}$$

$$U^{-}_{k+1}=U_{k+3/2,l+1/2}-1/2\Delta x U_{x,k+3/2,l+1/2}-1/2\Delta y U_{y,k+3/2,l+1/2}$$

$$U_{x,k+1/2,l+1/2}=\min\mathrm{mod}(U_{x,k,l+1/2},U_{x,k+1,l+1/2})$$

$$U_{y,k+1/2,l+1/2}=\min\mathrm{mod}(U_{y,k,l+1/2},U_{y,k+1,l+1/2})$$